JOURNAL OF MATERIALS SCIENCE 6 (1971) 1197–1203

Fracture Energy of an Epoxy Composite System

F. F. LANGE, K. C. RADFORD
Westinghouse Research Laboratories, Pittsburgh, Pennsylvania 15235, USA

Fracture energy data are presented for an epoxy-alumina trihydrate composite system in which both the volume fraction and particle size of the dispersion were changed. These data show that the fracture energy of a brittle epoxy composite can be significantly increased by choosing the proper volume fraction and particle size of the dispersed second phase. The results are discussed in terms of several mechanisms which could account for the observed increase in fracture energy. A recently proposed mechanism of crack interaction with a second phase dispersion is qualitatively consistent with these results.

1. Introduction

Fracture energy is one of three factors that are believed to govern the strength of materials. Although the two other factors are equally important; viz. the material's elastic properties and the size of the crack from which failure initiates [1], this article will only be concerned with the fracture energy of a brittle epoxy composite material.

Recently it was suggested that the fracture energy of a brittle material could be increased by incorporating a second phase dispersion [2]. To test the validity of this suggestion, fracture energy experiments were conducted on an epoxy resin in which particles of alumina trihydrate were dispersed.

Data were obtained for various epoxy-dispersion combinations in which both the particle size and the volume fraction of the alumina trihydrate dispersion were changed. In this manner, the experimental relation between the fracture energy and interparticle spacing was obtained. A summary of other mechanical properties of this system is given elsewhere [3].

2. Material Preparation

The epoxy system used in this investigation was a liquid diglycidyl ether of bisphenol A (ERL 2774)* cured with HHPA* in the ratio 100:80; 0.18% accelerator (DMP 10)* was added. The dispersed second-phase material was an alumina trihydrate powder which was obtained with average particle sizes of 1, 8 and 12 μm.†

Batches were made with 0.10, 0.215 and 0.295 volume fraction (VF) of each of the three different powders. A batch with 0.03 VF of 1 μm and batches with 0.43 VF of 8 and 12 μm powders were also made. Each batch was mixed at 100°C with a high-speed stirrer for several hours before de-airing and casting into a block mould with dimensions of 7 × 7 × 1.25 in. The castings were cured at 100°C overnight and post-cured at 135°C for 6 h. In this investigation, the densities of the resin and the alumina trihydrate were taken as 1.17 and 2.47 g/cc, respectively.

3. Fracture Energy Determination

Many different specimen configurations are acceptable for the measurement of fracture energy [4]. Regardless of the specific configuration,the fracture energy is determined by measuring the force (F) required to propagate an existing sharp crack within a specimen. Knowing this force, the elastic modulus (E) of the material, the length of the crack (L), and the specimen dimensions, the fracture energy can be calculated using a standard equation derived for the particular specimen geometry. Since these equations were derived assuming brittle fracture conditions, certain limitations on the specimen size must be maintained to ensure a brittle mode of fracture.

*ERL 2774 is a product of Union Carbide Corporation, HHPA was obtained from Allied Chemical, and DMP 10 from Rohm and Haas.
†All powders were obtained from Alcoa Corporation.

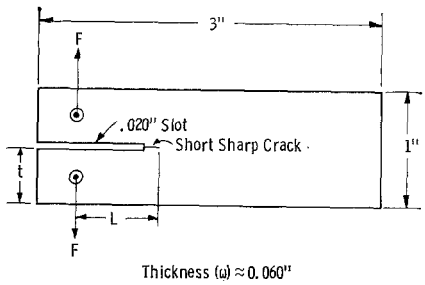

Figure 1 Schematic diagram of a double beam cantilever specimen.

Fig. 1 shows the double-beam cantilever specimen configuration used in this investigation. The equation used to calculate the fracture energy for this configuration was derived by both Gross and Srawley [5] and Wiederhorn *et al* [6], who used a linear elastic solution with the appropriate boundary conditions. The fracture energy can be determined from the following equation:

$$FE = 6F^2L^2/Ew^2t^3[1 + 1.32\,t/L + 0.542(t/L)^2]. \quad \ldots\ldots(1)$$

Weiderhorn found that this equation was valid when the ratio of the crack length (L) to beam width (t) was greater than 1.5.

The specimen thickness (w) must be large enough to prevent what is known as a shear type fracture. This has been discussed elsewhere [4], but briefly, the specimen width must be much larger than the radius of the plastic zone at the crack tip. Once this condition is satisfied, as it was for these experiments, the measured energy absorption is that required to initiate failure and not that required to deform a large volume of the material.

Specimens were machined from the large blocks of the cast epoxy-dispersion material with dimensions as given in fig. 1. A slot was also machined as shown, so that each specimen had a similar crack length. A sharp crack was extended a short distance beyond the end of the slot by tapping a razor blade gently into the specimens. The ends of these cracks were observed with a microscope at low magnification.

The specimens were loaded in tension to failure using an Instron testing machine. The load was transmitted to the specimens by "S" hooks placed through the holes; each hook had sufficient freedom to self-align under small loads. The cross-head rate was held constant at 0.05 cm/min. Each specimen was tested within a few hours after introducing the sharp crack. All compositions were tested at both room temperature and 77°K (immersed in liquid nitrogen).

Reproducibility of the fracture energy data was measured by testing different castings of the same composition. Double beam cantilever tests were also repeated on the same batches after periods of up to a year.

The elastic moduli (necessary for determining the fracture energies) of these composites were determined at both room temperature and 77°K by fixing strain gauges to rectangular shaped specimens which were placed in tension. These measurements were conducted on the epoxy composites containing the 8 μm alumina trihydrate dispersion. It has been shown [3] that at constant volume fraction, particle size does not affect the elastic modulus.

Examinations of the fractured surfaces were made using both a scanning electron microscope and an optical microscope.

4. Results

4.1. Fracture Energy

The reproducibilities of the calculated fracture energies both between different batches of the same composition and the same batch composition tested on different dates are given in table I. The extent of the scatter in these data is small considering the many variables that could change during the fabrication (e.g. curing time and temperature, hardener additions, etc.) and testing (specimen ageing, humidity, etc.). This scatter is also small relative to the change in fracture energy as a function of both the volume fraction and particle size of the second phase dispersion. Thus, high confidence was placed in the relative values of the fracture energy data between the different composite compositions.

Table II summarises the fracture energy data for all the different composite compositions investigated. Figs. 2 and 3 illustrate these results in graphical form. The principal results can be summarised as follows:

(1) At room temperature, a significant increase in the fracture energy occurred for each of the three composite series. At 77°K, this increase was not as large.

(2) A fracture energy maximum occurred in all cases except for the 1 μm composite series at 77°K.

(3) At both temperatures, the greatest fracture energy was obtained for the composite series

TABLE I Fracture energy reproducibilities within batches and between batches of the same composition

(a) Within Batches

Composition	Test Date	Fracture energy (ergs/cm²)	
		RT	Liq N_2
Unfilled	7–31–69	95 400 ± 8.1%	154 800 ± 15.2%
	5–14–70	77 600 ± 7.2	187 000 ± 10.4
8 μm 0.10 VF	7–31–69	171 700 ± 18.0	
	8–11–69	181 800 ± 18.2	
12 μm 0.295 VF	7–31–69	195 700 ± 1.8	
	5–15–70	204 400 ± 5.4	

(b) Between Batches

Composition	Batch number	Fracture energy (ergs/cm²)	
		RT	Liq N_2
Unfilled	2–24–69	95 400 ± 8.1%	154 800 ± 15.2%
	5–5–69		184 200 ± 14.2
	12–27–68		165 000 ± 6.8
	12–10–68		143 700 ± 7.7
	11–19–68	98 600 ± 12.8	
	12–2–68	89 600 ± 25.2	
8 μm 0.43 VF	2–20–69	109 000 ± 15.5	149 400 ± 3.3
	1–28–69	117 000 ± 16.2	155 200 ± 10.1

containing the largest average particle size dispersion (12 μm).

It should also be noted that the fracture energy of this epoxy (without a dispersion) increased as the temperature decreased. An analogous situation occurs for glasses [7] and polycrystalline ceramics [8].

4.2. Fracture Surface Topography

Two different types of fracture surfaces were observed. One type included surface steps associated with each particle encountered by the moving crack front (see fig. 4a). Similar steps have been observed by others, and they are a characteristic feature of the interaction of a crack

TABLE II Tensile modulus and fracture energies at room temperature and 77°K

Volume fraction dispersion	Tensile modulus × 10^{10} dynes/cm²	Fracture energy (ergs/cm²)		
		1 μm	8 μm	12 μm
		Room temperature		
0	3.80	95 400 ± 8.1%		
0.03	3.85	132 900 ± 16.0%		
0.10	4.14	130 600 ± 16.2	171 700 ± 18.0%	242 000 ± 6.4%
0.215	5.52	65 000 ± 30.5	206 000 ± 5.1	281 000 ± 3.8
0.295	6.55	67 300 ± 14.3	176 500 ± 9.5	195 700 ± 1.8
0.43	8.96		109 000 ± 15.5	125 000 ± 15.9
		Liquid nitrogen (77°K)		
0	10.36	165 000 ± 6.8%		
0.03	10.45	89 600 ± 6.7%		
0.10	11.40	111 800 ± 11.3	209 000 ± 16.4%	189 500 ± 3.9%
0.215	12.10	92 800 ± 23.7	171 000 ± 3.9	202 200 ± 6.8
0.295	15.20	69 700 ± 16.0	148 000 ± 17.3	159 000 ± 8.3
0.43	16.10		149 400 ± 3.3	128 600 ± 11.6

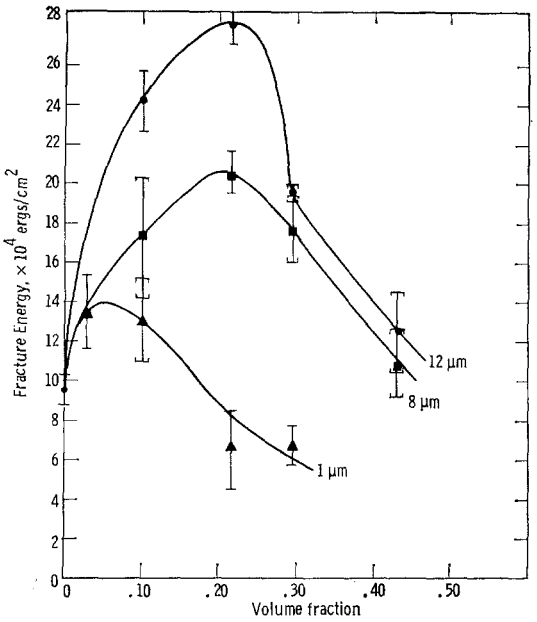

Figure 2 The relation between fracture energy and dispersion volume fraction at room temperature.

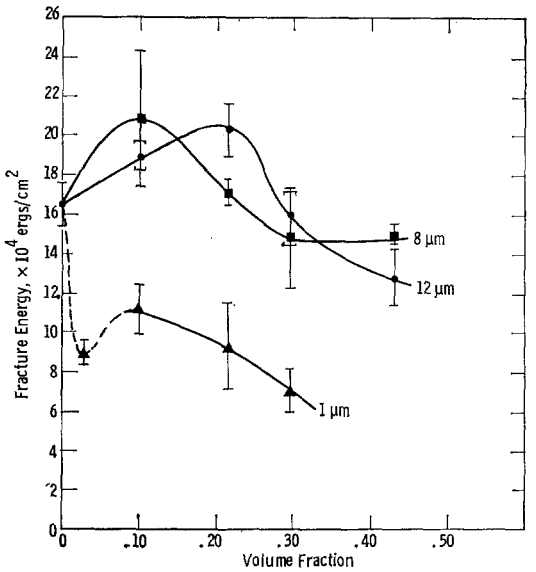

Figure 3 The relation between fracture energy and dispersion volume fraction at 77°K.

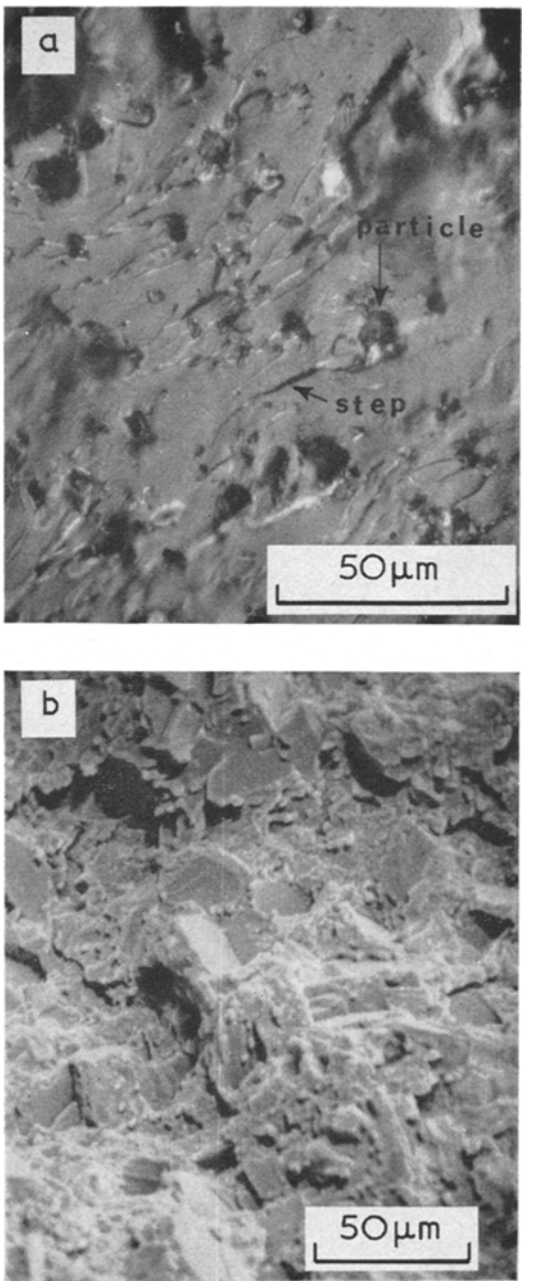

Figure 4 Fracture surface topography of two epoxy-dispersion composites: (a) 12 μm, 0.10 volume fraction composite showing steps that are characteristic of the interaction of a crack front with inhomogeneities; (b) 8 μm 0.40 volume fraction showing the polycrystalline nature of the fracture surface.

with inhomogeneities such as voids [9] and second phase particles [10]. This type of surface was only observed for composites containing volume fractions of the dispersed phase which were smaller than those resulting in a maximum fracture energy.

The second type (see fig. 4b) of fracture surface appeared similar to that of a polycrystalline material. The epoxy matrix and the alumina trihydrate particles were nearly indistinguish-

able, and no steps were associated with the particles. Such surfaces were found for all composites containing volume fractions larger than those resulting in a maximum fracture energy.

A combination of both types of fracture surface was observed for composites whose fracture energy was a maximum. For these surfaces steps were observed adjacent to most particles, but these steps usually intercepted the neighbouring particles.

In general, for large interparticle spacings, a surface containing steps was observed. For small interparticle spacings, the surface appeared polycrystalline.

Scanning electron microscopy revealed that particles intercepted by the crack front fractured in an irregular manner. In most cases,the fracture surfaces of these particles were not planar with the epoxy surface. Although the appearance of the particle fracture surfaces was consistent with a cleavage mode (indicating transparticle fracture it was uncertain whether cleavage or fracture along the epoxy-particle interface actually occurred.

5. Discussion

Several conclusions can be drawn from the above results concerning the effect of the second phase dispersion on the fracture energy:

(1) At 77°K, the second phase dispersion has less effect than it does at room temperature.

(2) There appears to be a relation between fracture energy, particle size, interparticle spacing, and fracture surface topography.

The first of these conclusions is difficult to explain without knowledge of the temperature dependence of the fracture energy of other epoxy-dispersion composite systems. The fracture energy of the epoxy by itself is observed to be significantly larger at 77°K than at room temperature. Since this material can be considerd brittle at both temperatures, the larger elastic modulus at 77°K (see table II) may be responsible for the increase in fracture energy; i.e in a homogeneous, single phase material, a higher elastic modulus means a stronger intermolecular bond, and therefore a greater energy is required to break the bonds during fracture. If it is assumed that the effect of the dispersion on the fracture energy is independent of temperature while the epoxy itself is strongly influenced by temperature, then the relatively small influence of the dispersion on the fracture energy at 77°K can be explained.*

The second conclusion, the inter-dependence between fracture energy, particle size, interparticle spacing, and fracture surface topography will be discussed with reference to several possible mechanisms:

(1) The effect of increased surface area (surface roughness) on the fracture energy.

(2) Energy absorption by the dispersed phase.

(3) The interaction between a crack front and the dispersed phase.

Surface roughness increases a material's fracture energy due to the increase in fractured surface area. This increase is independent of particle size and only depends on volume fraction of the dispersed phase. The contribution of this mechanism to the fracture energy cannot be determined absolutely, but the maximum possible contributions can be estimated. This was done by using a model which describes the fracture surface as a plane with raised cubes representing the dispersed particles. The maximum increase in surface area (and hence fracture energy) is only 10% for 0.10 volume fracture and rises to less than 150% for 0.50 volume fraction. Thus, the observed increase in fracture energy cannot totally be due to surface roughness because (a) predicted fracture energy increases are much less than those observed, and (b) both the observed particle size dependence and the occurrence of a maxima in the data cannot be explained by this mechanism.

The fracture energy of a material may be increased if the dispersed phase absorbs energy during fracture (e.g. by plastic deformation). Although the authors suspect that alumina trihydrate is a brittle material with a lower fracture energy than the epoxy (no fracture energy data for this material are available), it is conceivable that this material may plastically deform during fracture. If this were the case, the fracture energy would continue to rise as the volume fraction of the dispersed phase was increased, without any maxima in the data. Thus, this mechanism does not explain the data.

The other possible mechanism that might be

*The authors would like to add the following comment made by the reviewer:
"In discussing the effect at 77°K, it is worth taking into account the fact that the microstresses in the composite, present as a result of the differential contraction of the resin and second phase, will be different at 77°K than at normal ambient temperatures."

responsible for the observed fracture energy data is the interaction of a crack with the second phase particles. Observations of such interactions have been described elsewhere [2], and can be summarised as follows. During fracture, a moving crack front (i.e. the periphery of a crack) is momentarily pinned at positions of inhomogeneities within the brittle matrix. This interaction leads to the bowing out of the crack front between the pinning positions, thus increasing its total length. On breaking away from these pinning positions, the crack front creates characteristic steps on the fracture surface. These steps are formed by the overlapping of the crack front as it bows between the dispersed particles.

Lange [2] has proposed that in order to create an increase in crack front length, an increase in strain energy is required which in turn leads to an increase in the material's fracture energy. His analytical model predicted that the fracture energy should increase as the dispersed particle spacing decreases, irrespective of the particle size.

The fracture energy results obtained here are in qualitative agreement with this proposed mechanism. The observation that fracture steps, which are associated with each particle form behind the moving crack front indicates that the crack front does bow between the dispersed particles. Also, as the particle spacing decreases, the fracture energy does rise. However, a maximum is reached which infers that the dispersed particles become too closely spaced for an effective crack front interaction. This is also inferred from the topography of the fracture surfaces, i.e. characteristic steps indicating crack interaction are no longer distinguishable once the maximum fracture energy is exceeded. As shown in fig. 5, prior to the fracture energy maximum, the increase not only depends on the interparticle spacing, but also on the particle size. This is not inconceivable because the effectiveness of the pinning positions should depend on the overlapping of the stress fields associated with the crack front as it moves both between and around the particles. Since these stress fields are inversely proportional to the square root of the distance from the crack front [11], the particle size, which separates the crack front segments, should influence the amount of bowing between the dispersion before the crack front breaks away. Thus, smaller particles will be less effective as pinning positions than larger particles. For a given interparticle spacing, therefore, the fracture energy should be larger for the composite containing the larger particles.

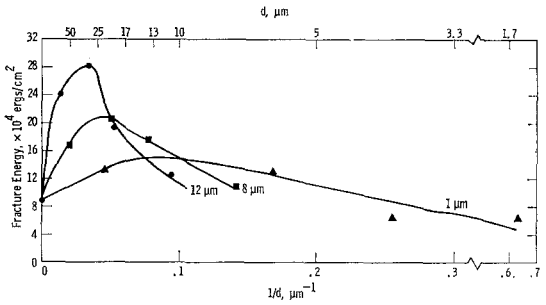

Figure 5 Relation between fracture energy and particle spacing at room temperature

$$\left(d = \frac{2D\,(1 - VF)}{3VF}\ ;\right.$$
$$\left.\begin{array}{l} d = \text{partial spacing} \\ D = \text{particle size} \\ VF = \text{volume fraction} \end{array}\right). \qquad [12]$$

It is the authors' opinion that this mechanism, i.e. the interaction of the crack with the second phase dispersion, most closely explains the data observed for this epoxy-alumina trihydrate composite system. It should also be noted that one of the authors (F. F. Lange)is also investigating another brittle composite system, viz. a glass-Al_2O_3 system. To date, similar results and conclusions have been obtained. Thus, the increase in fracture energy due to a second phase dispersion may be a general phenomenon which occurs for many brittle materials.

Acknowledgement

The authors are grateful for the support and interest of D. E. Harrison.

References

1. A. A. GRIFFITHS, *Phil. Trans.* **221A** (1920) 163.
2. F. F. LANGE, *Phil. Mag.* **22** (1970) 983.
3. K. C. RADFORD, to be submitted to *J. Mater. Sci.*
4. W. F. BROWN, JR. and J. E. SRAWLEY, ASTM Special Tech. Pub. No. 410, (1966).
5. B. GROSS and J. E. SRAWLEY, NASA TND-3295 (February 1966).
6. S. M. WIEDERHORN, A. M. SHORB, and R. L. MOSES, *J. Appl. Phys.* **39** (1968) 1569.
7. S. M. WIEDERHORN, *J. Amer. Ceram. Soc.* **52** (1969) 99.
8. P. L. GUTSHALL, G. E. GROSS, and G. D. SWANSON, Tech. Rept.
9. H. BETHGE, *Phys. Stat. Sol.* **2** (1962) 814.

10. S. M. OHLBERG, H. R. GOLOB, and C. M. HOLLABAUGH, *J. Amer. Ceram. Soc.* **45** (1962) 1.
11. M. L. WILLIAMS, *J. Appl. Mech. Trans. ASME* **24** (1957) 109.
12. R. L. FULLMAN, *J. Metals Trans AIME* **197** (1953) 447.

Received 18 March and accepted 19 April 1971.